environmental microbiology

Environmental Microbiology (2019) **00**(00), 00–00 doi:10.1111/1462-2920.14731

A common mechanism for efficient N_2O reduction in diverse isolates of nodule-forming bradyrhizobia

Daniel Mania,[1*] **Kedir Woliy**,[1] **Tulu Degefu**[1,2] **and Åsa Frostegård**[1*1*]

[1]*Faculty of Chemistry, Biotechnology and Food Science, Norwegian University of Life Science, Ås, Norway.*

[2]*International Crops Research Institute for the Semi-Arid Tropics, Addis Ababa, Ethiopia.*

Summary

Bradyrhizobia are abundant soil bacteria, which can form nitrogen-fixing symbioses with leguminous plants, including important crops such as soybean, cowpea and peanut. Many bradyrhizobia can denitrify, but studies have hitherto focused on a few model organisms. We screened 39 diverse *Bradyrhizobium* strains, isolated from legume nodules. Half of them were unable to reduce N_2O, making them sources of this greenhouse gas. Most others could denitrify NO_3^- to N_2. Time-resolved gas kinetics and transcription analyses during transition to anaerobic respiration revealed a common regulation of *nirK*, *norCB* and *nosZ* (encoding NO_2^-, NO and N_2O reductases), and differing regulation of *napAB* (encoding periplasmic NO_3^- reductase). A prominent feature in all N_2-producing strains was a virtually complete hampering of NO_3^- reduction in the presence of N_2O. In-depth analyses suggest that this was due to a competition between electron transport pathways, strongly favouring N_2O over NO_3^- reduction. In a natural context, bacteria with this feature would preferentially reduce available N_2O, produced by themselves or other soil bacteria, making them powerful sinks for this greenhouse gas. One way to augment such populations in agricultural soils is to develop inoculants for legume crops with dual capabilities of efficient N_2-fixation and efficient N_2O reduction.

Introduction

Rhizobia are known for their capacity to fix atmospheric dinitrogen (N_2) into biologically available ammonia (NH_3). Symbiotic associations between crop and fodder legumes and rhizobia account for 75 % – 84 % of the biologically fixed nitrogen in agricultural systems, with estimates varying between 225 and 342 kg N ha^{-1} $year^{-1}$, compared to <73 kg N ha^{-1} $year^{-1}$ fixed by other plant associated or free-living bacteria (Herridge *et al*., 2008). In their N_2 fixing symbiosis with legume plants, rhizobia increase the supply of nitrogen to soils and thereby the yield of other, non-legume crops, when used in intercropping systems or crop rotations, thus reducing the need for mineral fertilizers. In addition, legumes provide a rich source of protein, and increased production is promoted by the authorities in many countries to secure livestock feed and food for rapidly growing populations. However, not every combination of plant host and microsymbiont results in equally efficient N_2 fixation. This specificity lies at the strain/cultivar level for bacteria and host plants, respectively (Thrall *et al*., 2011). To fully realize the potential of symbiotic N_2 fixation, there is a need to develop a range of compatible and effective inoculants as biofertilizers for different legume crops. This requires the establishment of biobanks of rhizobial strains that are well characterized and tested for efficacious nodulation with existing and novel legume varieties.

The genus *Bradyrhizobium* comprises many strains that can form symbiotic root nodules with economically and nutritionally important legume species like soybean *(Glycine max)*, peanut *(Arachis hypogaea)*, cowpea (*Vigna unguiculata*) and Bambara groundnut (*Vigna subterranea*). In addition to their ability to fix N_2, some *Bradyrhizobium* strains are also known to denitrify NO_3^- or NO_2^- stepwise to NO, N_2O and/or N_2, in order to support respiratory ATP production in the absence of O_2 (Bedmar *et al*., 2005; Siqueira *et al*., 2017). Denitrification is likely to increase the fitness of free-living cells of *Bradyrhizobium* strains under periods of anoxia. Several studies also report denitrification by *Bradyrhizobium* bacteroids inside nodules (Sánchez *et al*., 2010; Hirayama *et al*., 2011), even though it remains to be elucidated if bacteroids contribute significantly to the total soil denitrification potential. So far, most detailed studies on the genetics and regulation of denitrification in bradyrhizobia have focused on the soybean microsymbiont *B. diazoefficiens* USD110, recently reclassified from the species *B. japonicum* (Delamuta *et al*., 2013). This strain possesses a complete denitrification pathway that includes periplasmic nitrate reductase NapAB but

Received 18 February, 2019; accepted 2 July, 2019. For correspondence. *E-mail daniel.mania@nmbu.no; Tel. (+47) 67232589; Fax (+47) 67230691. **E-mail asa.frostegard@nmbu.no; Tel. (+47) 67232473; Fax (+47) 67230691.

not the membrane-bound NarG (Delgado *et al*., 2003), copper-containing nitrite reductase NirK (Velasco *et al*., 2001), cytochrome *c* dependent nitric oxide reductase cNor (Mesa *et al*., 2002) and nitrous oxide reductase NosZ, encoded by the genes *napAB*, *nirK*, *norCB* and *nosZ* (Velasco *et al*., 2004). NO and N_2O are intermediate products of denitrification that are released, if the organisms do not reduce these gases fast enough, or when strains have a truncated denitrification pathway from which genes encoding NorCB and/or NosZ are absent (Shapleigh, 2013). Although some early studies demonstrated that several strains belonging to the genus *Bradyrhizobium* (then named *Rhizobium*) and some other groups of rhizobia were able of complete or partial denitrification (Daniel *et al*., 1982), information about how widespread this trait is among bradyrhizobia is still ambiguous. In the present study, we investigated a diverse collection of *Bradyrhizobium* strains, isolated from various legume nodules, for their regulation of denitrification and their capacity to reduce N_2O.

Denitrification in agricultural soils is a major producer of the prominent greenhouse gas N_2O (Montzka *et al*., 2011; Reay *et al*., 2012), and there is an explicit need to develop novel methods to curb these emissions, as recently expressed in the last special report by IPCC (Rogelj *et al*., 2018). Hotspots for denitrification are likely to occur in legume fields when nodules die, or when the host plant dies after harvesting, releasing carbon and nitrogen into the surrounding soil. This, in turn, will stimulate microbial growth and nitrification of NH_4^+, leading to increased NO_3^- and NO_2^- concentrations and depletion of O_2. When conditions become anoxic, denitrifying organisms in the surrounding soil, including rhizobial cells released from the decomposing nodules, will reduce the NO_3^- and/or NO_2^- to nitrogen gasses (Yang and Cai, 2005; Akiyama *et al*., 2016). In view of this, *Bradyrhizobium* strains that are used as biofertilizers for leguminous crops should be screened for their ability to reduce N_2O to N_2, since they as free-living cells, possibly released from decaying nodules, can potentially mitigate the emission of N_2O produced by themselves or by surrounding organisms (Itakura *et al*., 2013; Akiyama *et al*., 2016).

The present work aimed to shed more light on the prevalence of denitrification among taxonomically diverse bacteria belonging to the genus *Bradyrhizobium* and the regulatory biology involved. We demonstrate that this group of organisms comprises several denitrification phenotypes, which vary in their intermediate and end products. High-resolution gas kinetics in combination with transcription analyses provided detailed information on how these organisms regulate the transition from aerobic respiration to denitrification and further growth during periods of anoxia, and suggest that some of these organisms can act as effective sinks for N_2O. We screened 39 *Bradyrhizobium* strains that are part of our biobank of rhizobia isolated from nodules of leguminous trees and herbs growing in Ethiopia (Wolde-Meskel *et al*., 2004). The strains were characterized phylogenetically and metabolically in earlier studies and classified into seven different genospecies (Wolde-meskel *et al*., 2004a, 2004b; Wolde-Meskel *et al*., 2005; Degefu *et al*., 2017). Among them, we identified several strains that carry complete denitrification pathways, thus potentially able to reduce NO_3^- all the way to N_2. Common to these strains was an apparent inhibition of NO_3^- reduction in the presence of N_2O. This was previously observed in *Bradyrhizobium japonicum* USDA 143 (Tucker and Neal, 1988) but has not yet been investigated in detail. To further examine the phenomenon, we chose one representative strain (AC87j1) from our collection and conducted detailed analyses of denitrification gas kinetics and transcription of *napA*, *nirK*, *norB* and *nosZ*. Like other, earlier sequenced strains of *Bradyrhizobium* (Delgado *et al*., 2003), this strain did not possess the membrane-anchored, dissimilatory nitrate reductase NarG. We hypothesize that NapC, transferring electrons to the periplasmic nitrate reductase NapAB, cannot compete for electrons with cytochrome bc_1, which supplies electrons to NirK, NorCB and NosZ via cytochrome *c* in the periplasm. Such a competition for electrons could have a role in balancing denitrification by throttling NO_3^- reduction when NO_2^-, NO and N_2O are abundant as electron acceptors, in order to avoid accumulation of cytotoxic NO_2^- and/or NO. The preference for N_2O reduction may be general to all denitrifiers carrying NosZ and NapAB but not the membrane-bound, cytoplasm-facing NarG, which receives electrons from the quinol pool via its own pathway encoded in the same operon. In the present study, the successful competition for electrons by NosZ appeared among widely diverse *Bradyrhizobium* strains, which holds promise for the development of a wide range of biofertilizer inoculants that are efficient nitrogen fixers with specific legumes, and which also act as strong sinks for N_2O.

Materials and methods

Bacterial strains and growth conditions

All *Bradyrhizobium* strains were taken from our own culture collection (Wolde-Meskel *et al*., 2004) and grown at 28 °C in Yeast Mannitol Broth (YMB) (Schwartz, 1972), consisting of 10 g l^{-1} D-Mannitol, 0.5 g l^{-1} K_2HPO_4, 0.5 g l^{-1} Yeast Extract (Merck), 0.2 g l^{-1} $MgSO_4 \cdot 7H_2O$ and 0.1 g l^{-1} NaCl. The pH was adjusted to 7.0 with HCl (1 M). The added amount of C-source comprised >200 times surplus of electron donor compared to electron acceptors throughout all incubations, thus ensuring that the electron donor was not depleted. Measurements after incubations showed that the pH of cultures never decreased below 7.0, thus confirming that N_2OR was not inhibited by low pH. Supplements like KNO_3 and KNO_2 were added as sterile filtrated solutions to the concentrations indicated in the text. All cultures were

grown in 120 ml medical flasks, filled with 50 ml medium and a Teflon-coated magnetic stirring bar. The culture flasks were sealed with a gas tight butyl rubber septum (Matriks AS, Norway) and air was removed by six repetitions of applying vacuum for 360 s and He overpressure for 30 s. The remaining He overpressure was released prior to injection of O_2 and/or N_2O. Stirring at 700 rpm ensured even dispersion of cells and ensured proper gas exchange between the liquid phase and the headspace of the flasks. Antimycin A, myxothiazol and N,N,N′,N′-tetramethyl-p-phenylenediamine (all obtained from Sigma-Aldrich®, Germany) were dissolved in 96% ethanol. Ascorbate (Sigma-Aldrich®) was dissolved in H_2O. Negative controls with a corresponding concentration of ethanol and/or ascorbate showed no significant effect of these chemicals on AC87j1 cultures.

Gas measurements

Culture flasks were placed in a semiautomatic incubation system (Molstad *et al*., 2007), and samples from the headspace were taken at intervals by an autosampler unit connected to a peristaltic pump. Standard gases were filled into evacuated and crimp-sealed medical flasks without medium. Overpressure was released after the flasks were acclimated at the temperature of the associated experiment. Gas samples were pumped into a gas chromatograph (Varian; 7890A GC, Agilent) for analysis of O_2, CO_2, N_2O and N_2. NO was measured by a chemiluminescence NOx analyser (M200E, Teledyne). Measurements for N_2 and for exogenous N_2O were mathematically compensated for the dilution that took place when sampling the headspace (Molstad *et al*., 2007). This mathematical compensation did not affect rate calculations. The initial quantity of exogenous N_2O was reduced by N_2O losses due to sampling in the presence of O_2 before N_2O reduction commenced. Therefore, small variations in the initial O_2 and N_2O concentration, as well as initial cell numbers of cultures, lead to significant variations in the initial N_2O, ranging from approximately 30 to 45 μmol N_2O * $flask^{-1}$. These variations did not affect the experimental outcome in any way. Concentrations of O_2 and NO in the liquid were calculated taking the solubility and the removal of O_2 from the headspace through bacterial respiration into account. To exclude gas production from a chemical reaction of NO_2^- with the medium, sterile YMB was incubated with 2 mM NO_2^-. No NO, N_2O or N_2 was detected after 100 h of incubation at 28 °C.

Wet chemistry

For NO_2^- and OD measurements, samples of 0.1 to 1 ml were taken through the rubber septum of flasks with a sterile syringe. NO_2^- was measured with a chemiluminescence NOx analyser (Sievers 280i, GE Analytical Instruments), after converting NO_2^- to NO by a reaction with I_3^- (Cox, 1980; MacArthur *et al*., 2007). Samples (10 μl) of bacterial cultures were analysed for NO_2^- immediately after sample taking. The standard curves covered a range of 0 to 2 mM NO_2^- and were strictly linear with an R^2 of 0.999. The optical density of cultures was measured at a wavelength of 600 nm (UV mini 1240, Shimadzu). The OD_{600} was converted to cell numbers by colony counting, which gave a conversion factor of 4.9E8 cells * ml^{-1} * $OD_{600}{}^{-1}$.

Transcription analysis

Samples of cultures were taken through the rubber septa of flasks with sterile syringes. To minimize the disturbance by sampling, each treatment (no N_2O and 1 ml N_2O) was incubated in two triplicates, amounting to six flasks per treatment. Samples were taken from one triplicate until the remaining culture volume in each flask reached 38 ml. The gas measurements from successive triplicates were combined to verify that they approximated the gas kinetics of undisturbed controls within the same experiment. In addition, sample volumes were reduced as the density of the cultures increased. Samples of cultures were centrifuged immediately (5′; 4 °C; 10,000 g), resuspended in RNAprotect Bacteria Reagent (Qiagen) and stored at −20 °C. Lysis and RNA extraction were performed with a kit (RNeasy® Mini, Qiagen). The lysate was incubated at 37 °C prior to RNA extraction, to solubilize polysaccharides.

DNA was removed by treatment with TURBO DNA-*free* (Ambion) in 50 μl volumes, using 20 μl nucleic acid extract. Before reverse transcription, the DNase-treated RNA was analysed for remaining gDNA by quantitative PCR with *nosZ* primers. Reactions were performed in a StepOnePlus real-time PCR cycler (Applied Biosystems), using SYBR Premix Ex Taq II (TaKaRa). The *nosZ* standard curve was linear (r^2 = 0.999) down to 34 copies per reaction (C_T 30.07); the PCR efficiency was >93%. All samples (2 μl template) had a C_T > 35 and failed the melting curve test (wrong T_M and multiple peaks), indicating the absence of template. The DNase-treated RNA was therefore considered free of genomic DNA.

The remaining RNA was reverse-transcribed using Maxima Reverse Transcriptase (Thermo Scientific). The cDNA was stored at −80 °C until QX200 Droplet Digital PCR (ddPCR™, Bio-Rad) was performed. Thawed aliquots of the cDNA were always used up within 8 h and kept at 4 °C or on ice. Primers (Table 1) were designed with Primer3Plus (Untergasser *et al*., 2007). The droplet florescence threshold was set close to that of positive droplets, to prevent false positives due to rain. The rain droplets were added to the clouds of negative droplets.

Table 1. Primer pairs used in this study.

Gene	Primer	Sequence (5′ to 3′)
napA	Forward	GGACATGAGCTATGACGAGTACG
	Reverse	GTTGTAGACGAGGTTGTTGCAC
nirK	Forward	TCGAGACCTGGTTCATCCGC
	Reverse	CGTCGTTCCACTTGCCTTCG
norB	Forward	GTGAACTACTACACCCACGGC
	Reverse	CGTGCACATGATCCAGAAGC
nosZ	Forward	TACGTCCCGGTCTCGAACAATC
	Reverse	CGGCTTGATCTTGTCGTCGAAC

The coefficient of variation (CV) for single ddPCR reactions was ≤2.5% for most samples.

Whole genome sequencing

B. japonicum AC87j1 was grown aerobically in YMB at 28 °C. Cells were harvested after approximately 6 days, and DNA was extracted by using a kit (QIAamp® DNA Mini, Qiagen). Samples were processed using the Nextera XT sample preparation kit and sequenced by MiSeq (Illumina) using the MiSeq reagent kit v3 for 300 × 2 paired end (PE) sequencing. Adapters and bar codes were trimmed from the sequence reads before further preprocessing by Trimmomatic (quality threshold 20). Assembly was done using SPAdes with contig length set to 500 and minimum read coverage of 2. The genome of *B. japonicum* AC87j1 was annotated and analysed with RAST and SEED (Aziz *et al*., 2008; Overbeek *et al*., 2014). Features of translated genes were analysed with BLASTP 2.6.0+ (Altschul *et al*., 1997). When available, predictions were checked by comparison to homologous proteins with validated function in the closely related *Bradyrhizobium diazoefficiens* USDA 110. This Whole Genome Shotgun project has been deposited at DDBJ/ENA/GenBank under the accession PTFE00000000. The version described in this paper is version PTFE01000000.

Results

Complete denitrification pathways were found in taxonomically diverse Bradyrhizobium strains

Thirty-nine *Bradyrhizobium* strains, isolated from nodules of leguminous trees and crops, were analysed for their denitrification end products. The geographic origin, host plant, and phylogenetic classification were described earlier (Woldemeskel *et al*., 2004a, 2004b;Wolde-Meskel *et al*., 2005). The isolates selected for the present study represented seven well-defined genospecies within the genus *Bradyrhizobium*, as determined by multilocus sequence analysis (MLSA) (Degefu *et al*., 2017). The bacteria were screened for their denitrification end products after batch incubation in YMB supplemented with 1 mM NO_3^-, and with initial amounts of 1% O_2 and 40 μmol N_2O in headspace. The phylogenetic position of the strains, based on an alignment of the *glnII* gene encoding glutamine synthetase, is shown in Fig. 1 (adopted from Degefu *et al*., 2017), together with information about their genospecies designation and denitrification end point. A complete list containing this information for all the tested isolates is given in Table S1. Most of the strains (34 out of 39) reduced NO_3^- to NO, N_2O or N_2, indicating that denitrification is a common trait among these organisms. Moreover, 20 of these 34 strains (59 %) were complete denitrifiers, able to perform all four denitrification steps, including the reduction of N_2O to N_2. All except six of the complete denitrifiers clustered in genospecies I in the *B. japonicum* superclade (Vinuesa *et al*., 2008; Ramírez-Bahena *et al*., 2009), with the closest-related reference species being *B. ottawaense*. This group was in turn related to, but clearly separated from, *B. diazoefficiens*, which has been the model organism for denitrification studies of bradyrhizobia (Mesa *et al*., 2003; Bedmar *et al*., 2005; Torres *et al*., 2014). Of the four other complete denitrifiers in the *B. japonicum* superclade, one belonged to genospecies II (closest reference species *B. canariense*), while three belonged to genospecies IV (closest reference species *B. ganzhouenze*). Of the five strains belonging to the *B. elkanii* superclade, there were two complete denitrifiers, strains AC87b3 and AC87L, both in genospecies VI. All strains that reduced N_2O were also able to reduce NO_3^-. Thirteen strains lacked the last denitrification step and reduced NO_3^- to N_2O. This phenotype was found among all the genospecies except VI. One strain, which occupied an independent branch in the phylogenetic tree and was thus designated as unclustered (U), accumulated NO above 1 μM in the liquid without further reduction. The remaining five strains, belonging to genospecies V, VI and VII, neither reduced the exogenous N_2O nor the provided NO_3^- or NO_2^- (the latter tested for three of the five strains) to gaseous products (Fig. 1 and Table S1).

N_2O inhibited NO_3^- reduction

Detailed gas kinetics during and after transition to denitrification were analysed for sixteen of the N_2 producing strains (Fig. 1; Supporting Information Figs. S1 and S2, Table S1). These strains represent genospecies I, II and IV in the *B. japonicum* superclade and genospecies VI in the *B. elkanii* superclade. Duplicate cultures were incubated in vigorously stirred flasks containing YMB supplied with NO_3^-, and with 1% O_2 and 40 μmol N_2O in the headspace. The 11 strains in genospecies I showed very similar gas kinetics (Supporting Information Fig. S1), exemplified by strain AC87j1 (Fig. 2A). They all reduced the provided NO_3^- and N_2O stoichiometrically to N_2, with low (nmol * $flask^{-1}$ levels) of NO accumulation. The most prominent feature was that the N_2 production showed a biphasic pattern.

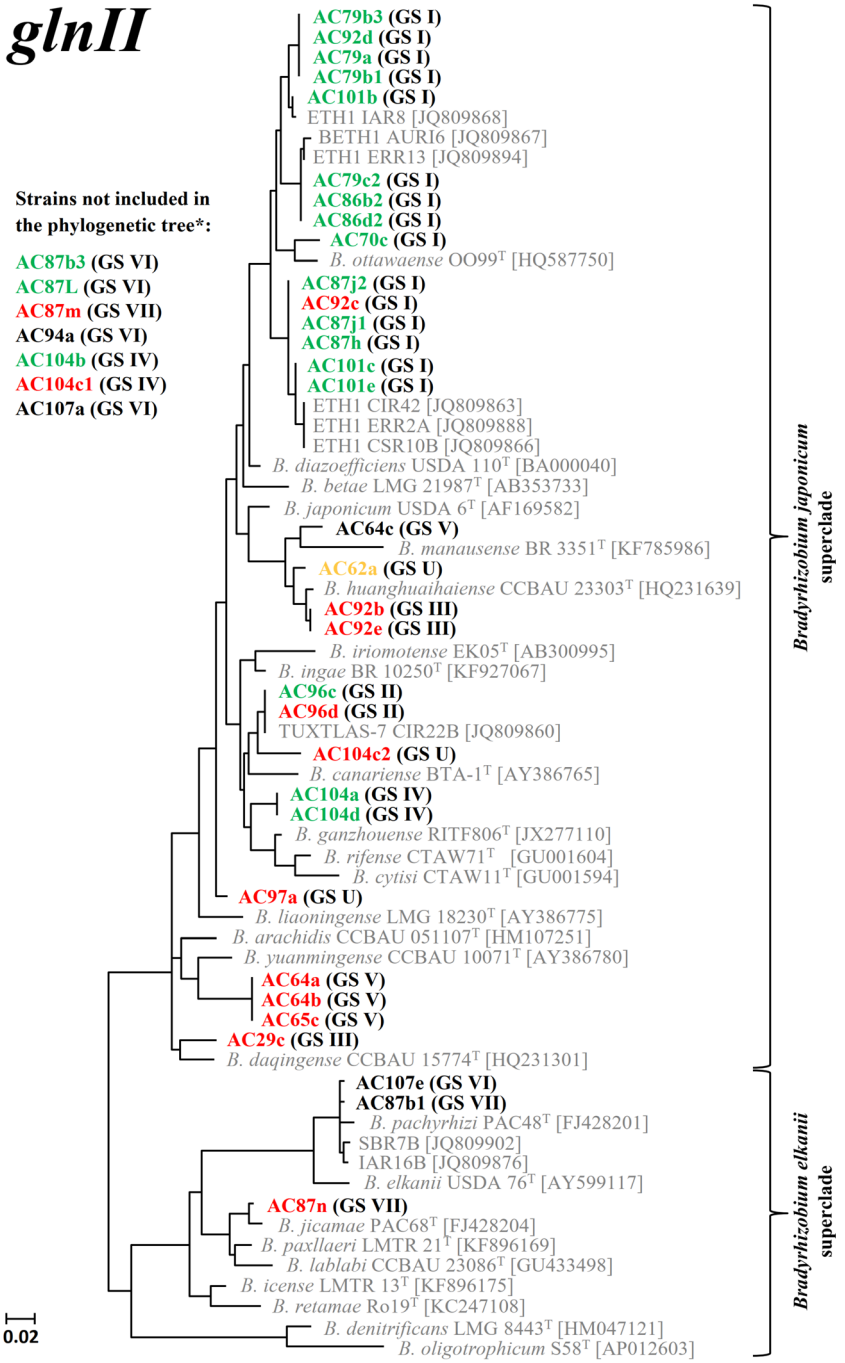

Fig. 1. Phylogenetic placement of *Bradyrhizobium* isolates tested for their denitrification end products. The tree was modified from Degefu *et al*. (2017). To determine if the strains were complete or partial denitrifiers, they were incubated anaerobically with NO_3^- and N_2O as electron acceptors. The strain names are coloured in accordance with their denitrification end products, as follows: Green: stoichiometrical reduction to N_2; Red: stoichiometrical reduction to N_2O; Yellow: partial reduction to NO. Strains in **black** font did not reduce NO_3^- and N_2O (strain AC87b1 did not reduce NO_2^- either). *denotes strains that were not included in the phylogenetic tree due to failure to amplify *glnII*. Information about their denitrification end product, and genospecies affiliation is found in Table S1. [Squared brackets] contain the GenBank accession number of *glnII*, encoding glutamine synthetase II, for each particular strain. (Round brackets) contain the genospecies (GS) designation based on consensus MLSA analyses (Degefu *et al*., 2017).

During the first phase, there was a rapid depletion of the exogenous N_2O. The quantity of N_2 produced per flask during this phase corresponded to the supplemented N_2O, and the maximum N_2O reduction rate of 10.10 $\pm$ 2.38 μmol N_2O-N * $flask^{-1}$ * h^{-1} matched the N_2 production rate of 10.14 $\pm$ 2.37 μmol N_2-N * $flask^{-1}$ * h^{-1}. This was a first indication that the presence of N_2O inhibited NO_3^- reduction. In comparison, the N_2 production rate after depletion of the exogenous N_2O was 2.07 $\pm$ 0.64 μmol N_2-N * $flask^{-1}$ * h^{-1}.

All eleven strains started to reduce the exogenous N_2O when the initially 10 μM O_2 in the liquid reached approximately 2 μM O_2. At the same time, a small and transient NO peak was observed that did not exceed low nanomolar concentrations. With the depletion of the exogenous N_2O, and with NO_3^- remaining as the only electron acceptor and source of N_2, the NO concentration increased to nanomolar concentrations again until the NO_3^- was depleted (as seen from the NO_3^- reduction rates as shown in Fig. 4A,

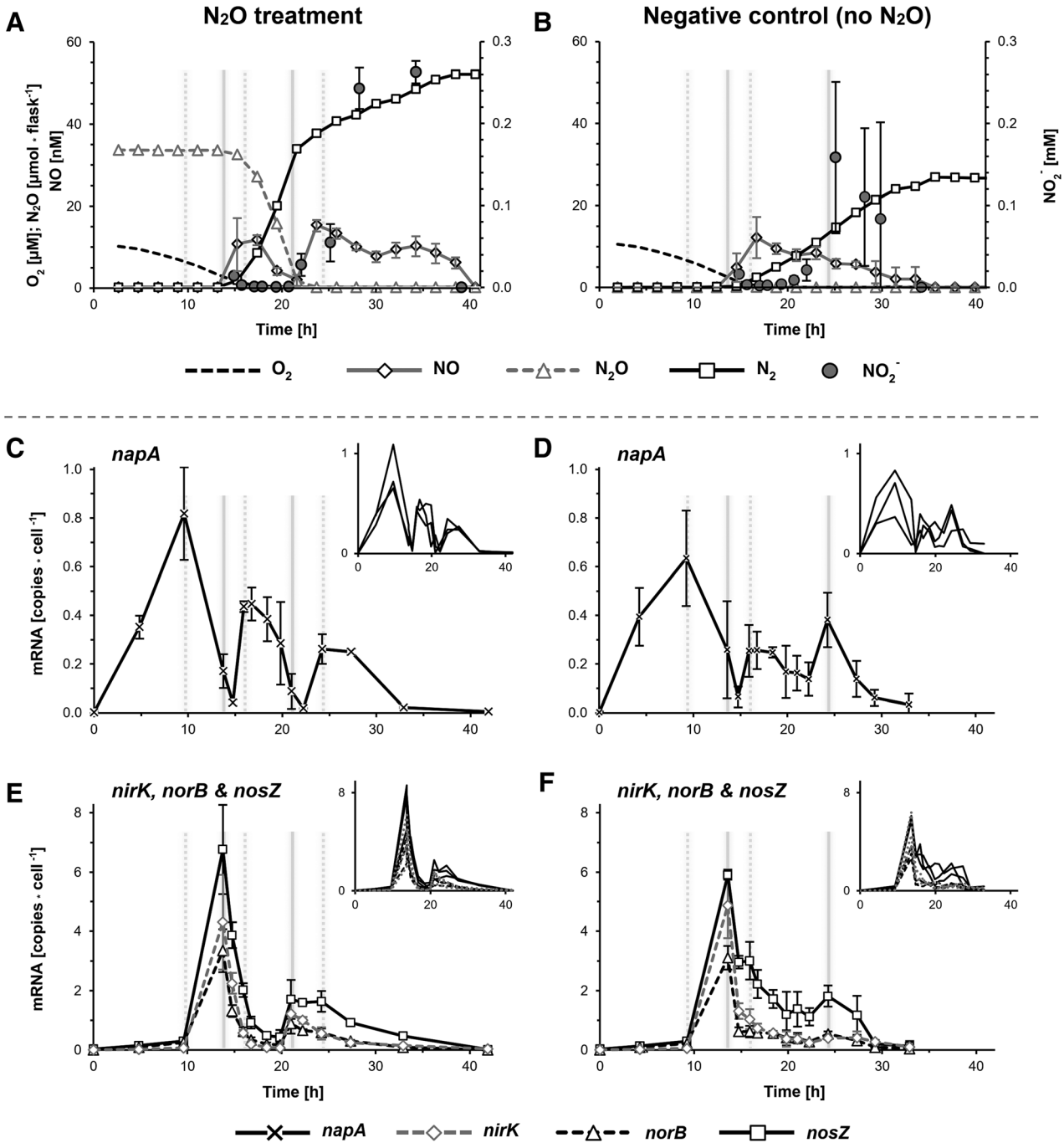

Fig. 2. Gas kinetics and NO_2^- concentrations (A & B) and mRNA copies * $cell^{-1}$ (C, D, E, & F) for *Bradyrhizobium* strain AC87j1 during and after transition from aerobic respiration to denitrification. The cultures were incubated in YMB supplemented with 1 mM NO_3^- (50 µmol), and with 1 ml initial O_2 in the headspace (approximately 10 µM in the liquid) and no or 40 µmol initial N_2O. Primer pairs (Table 1) for ddPCR™ targeted *napA*, encoding periplasmic NO_3^- reductase (C & D); *nirK*, encoding copper containing NO_2^- reductase (E & F); *norB*, encoding cytochrome *b* subunit of NO reductase (E & F); and *nosZ*, encoding clade I N_2O reductase (F & F). Error bars for NO and NO_2^- show standard deviations (n = 3). Error bars for O_2, N_2O, & N_2 were omitted; the standard deviation was ≤0.3 µM for O_2, ≤ 1.5 µmol * $flask^{-1}$ for N_2O, and ≤ 3 µmol * $flask^{-1}$ for N_2. Small charts show mRNA copy numbers of individual flasks. Grey vertical lines indicate upregulation of *napA* (dotted lines) or *nirK*, *norB*, and *nosZ* (solid lines) and link these events to the gas data for convenience.

calculated from measured NO_2^- production and the difference between N_2O reduction and N_2 production rates). Cultures that were not provided with exogenous N_2O started denitrification at a similar O_2 concentration as flasks with exogenous N_2O. The rate of N_2 production was similar to the rate in the second phase observed in flasks with

exogenous N_2O (Table 2; Fig. 2B). To determine if the inhibition of NO_3^- reduction by N_2O was exerted on the protein level, cultures of strain AC87j1, that had depleted the exogenous N_2O and actively reduced NO_3^- to N_2, were treated with a second injection of N_2O (Fig. 3). The slow N_2 production from NO_3^- increased instantaneously and matched the rate of N_2O reduction (Table 2), which provides further evidence for a strong preference for N_2O over NO_3^- in these organisms.

We also investigated whether exogenous N_2O inhibits NO_2^- reduction in the same way as seen for NO_3^- reduction (Fig. 4B; Table 2). Incubations with 1 mM NO_2^- instead of NO_3^- showed a 20% slower N_2 production. No change in pH was observed in the cultures incubated with NO_2^- (pH was 7.0 both at the start and at the end of the incubation), thus this slowdown of N_2 production was probably caused by NO_2^- toxicity. In the presence of exogenous N_2O, the N_2 production rate was higher than the N_2O reduction rate (Table 2), indicating simultaneous reduction of exogenous N_2O and NO_2^-. The calculated NO_2^- reduction rate in the presence of N_2O was 1.60 ± 0.19 μmol NO_2^--N * $flask^{-1}$ * h^{-1} (n = 10). Like the NO_3^- treatments, the NO_2^- treatments accumulated NO at low nanomolar concentrations during the reduction of the exogenous N_2O, further supporting the assumption that NO_2^- reduction was ongoing in the presence of N_2O.

The five N_2 producing isolates, which belong to genospecies other than genospecies I, displayed various denitrification phenotypes (Supporting Information Fig. S2). Strains AC96c (genospecies II) and AC104a and AC104b (genospecies IV), also belonging to the *B. japonicum* superclade, had a less stringent control of NO compared to the genospecies I strains, with rapid accumulation of NO to micromolar concentrations upon O_2 depletion. The problem of NO accumulation (4–8 μM) was seen in both duplicates of the AC104b culture, but only in one of the AC104a cultures, indicating that this is a stochastic phenomenon (Supporting Information Fig. S2). The AC104a culture that managed to keep the NO low showed the characteristic, biphasic N_2 production observed in all genospecies I strains. The reduction of exogenous N_2O to N_2 stopped when NO accumulated to high levels, while the reduction of NO_3^- to NO and N_2O continued, most clearly seen for AC104b (Supporting Information Fig. S2, left panel). Similar kinetics were found for strain AC96c, although the accumulation of NO following O_2 depletion was short-lived (Supporting Information Fig. S2). The apparent inhibition of N_2O reduction by NO in all these strains was overcome when the cultures managed to decrease the NO to nanomolar concentrations again. Albeit noteworthy, the inhibition of N_2O reduction by NO concentrations higher than 1 μM, which was observed in other bacteria before (Frunzke and Zumft, 1986), was not investigated further in this work. The two strains AC87b3 and AC87l, both in genospecies VI in the *B. elkanii* superclade, performed a very slow reduction of N_2O to N_2, which made it impossible to judge if exogenous N_2O inhibited NO_3^- reduction.

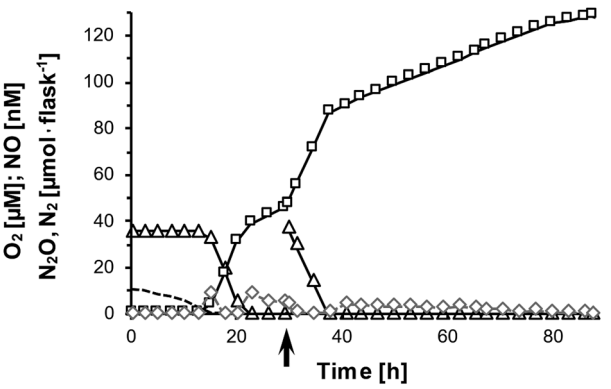

Fig. 3. Gas kinetics for *Bradyrhizobium* strain AC87j1 during and after transition from aerobic respiration to denitrification. The cultures were incubated in YMB supplemented with 1 mM NO_3^- (50 μmol) and with 1 ml initial O_2 in the headspace (approximately 10 μM in the liquid) and no or 40 μmol initial N_2O. After depletion of the initial N_2O, and during reduction of NO_3^- to N_2, cultures were treated with a second injection of approximately 40 μmol N_2O (29 hpi; marked by arrow). Standard deviations (n = 3) are smaller than the symbols and therefore not shown.

Transcriptional regulation did not explain the preference for N_2O reduction

To shed light on the transcriptional regulation of denitrification in bradyrhizobia and to investigate whether this may hold additional clues to understand the observed rapid N_2O reduction, a number of more detailed analyses were

Table 2. Rates of N_2O reduction and N_2 production in different treatments.

	In presence of exogenous N_2O		After N_2O depletion
	N_2O reduction	N_2 production	N_2 production
Treatment	[μmol N × $flask^{-1}$ × h^{-1}]		
NO_2^- and N_2O	6.9 ± 0.6	8.5 ± 0.5	3.3 ± 0.3
NO_3^- and N_2O	10.8 ± 0.1	10.8 ± 0.1	2.1 ± 0.0
Second injection of N_2O during NO_3^- reduction	10.0 ± 0.6	10.0 ± 0.5	1.8 ± 0.0
NO_3^- & N_2O; acetylene inhibition of N_2OR[a]	−5.0 ± 0.0	(not applicable)	(not applicable)

a. Only duplicates; negative value reflects N_2O production.

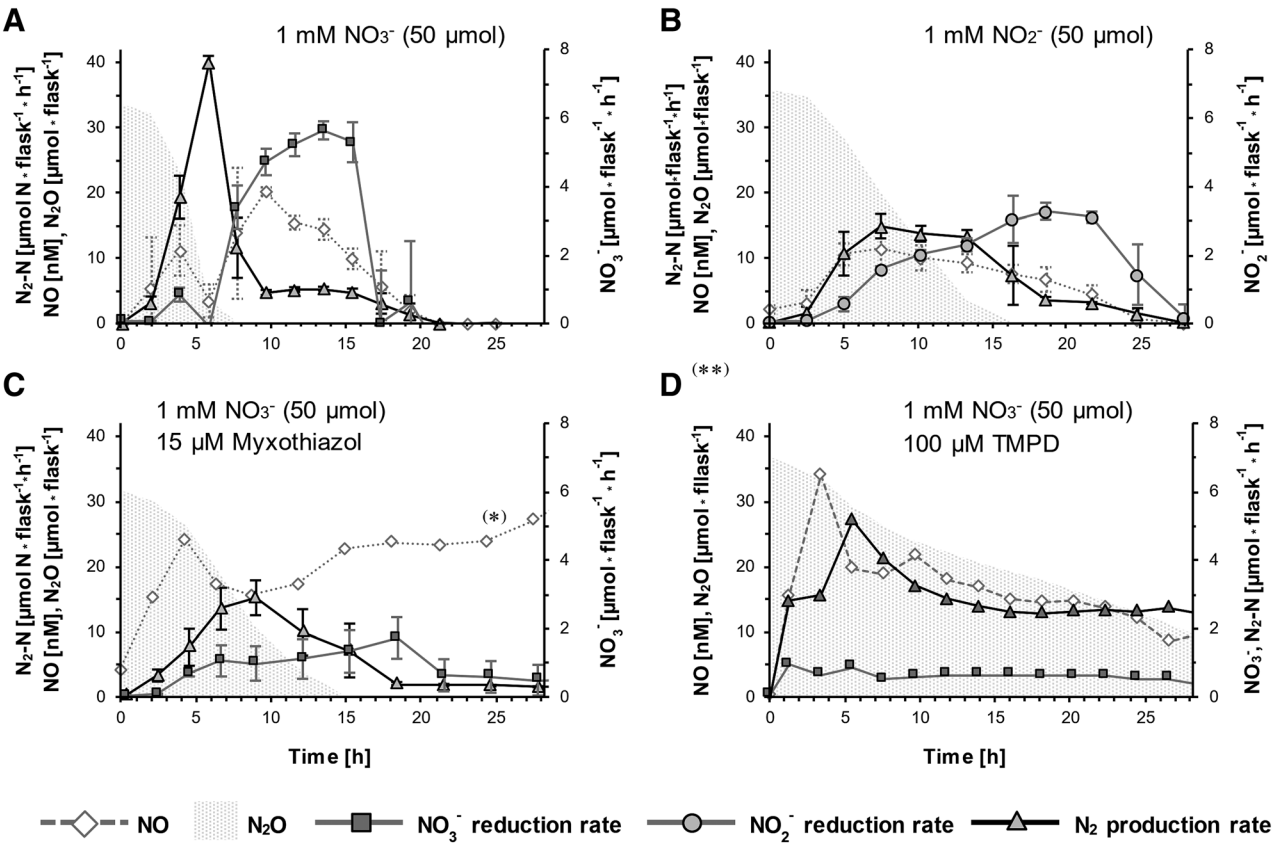

Fig. 4. Gas kinetics for *Bradyrhizobium* strain AC87j1 after transition from aerobic respiration to denitrification. The cultures were incubated in YMB supplemented with 1 mM (50 µmol) NO_3^- (A, C, and D) or NO_2^- (B), and with 1 ml initial O_2 in the headspace (approximately 10 µM in the liquid) and 40 µmol initial N_2O. A treatment with 15 µM myxothiazol (C) should hinder electron flow to the cytochrome bc_1 complex and further to NIR, NOR, and N_2OR; a treatment with 100 µM TMPD and 10 mM ascorbate (D) should reduce cytochrome *c* and thereby deliver electrons to NIR, NOR, and N_2OR, bypassing the cytochrome bc_1 complex. The NO_3^- and NO_2^- reduction rates were calculated from measured NO_2^- production and the difference between N_2O reduction and N_2 production rates. Diagrams start at the time point when O_2 was depleted (≤ 2 µM in the liquid) and when N_2O reduction started. Error bars show standard deviations (n = 3). (*) Error bars for NO in (C) were omitted due to high NO variations between replicate flasks. (**) Shown is one flask of a triplicate. Reduction of NO_3^- and N_2O took place concomitantly in all three replicates, as expected, but the rates differed in the three flasks. The chosen flask shows an intermediate effect of TMPD that is less/more pronounced in the other two flasks of the triplicate. For more details, see main text.

performed. For these, we arbitrarily chose one of the strains (strain AC87j1) among those which did not show problems with NO control, as a representative for the complete denitrifiers among our *Bradyrhizobium* strains. The number of mRNA copies per cell was determined at time intervals during incubation, using droplet digital PCR and primers targeting denitrification genes (Table 1). The inoculum was raised for several generations under aerobic conditions with vigorous stirring. This secured that the cells did not induce anaerobic respiration, seen from the number of denitrification gene transcripts, which was <0.03 mRNA copies * $cell^{-1}$ immediately after inoculation.

Cultures were incubated under standard conditions with 1 mM NO_3^- (50 µmol NO_3^-) and 1 ml N_2O (approximately 40 µmol N_2O) (Fig. 2). Transcription of *napA* during the incubation was generally one order of magnitude lower than that of *nirK*, *norB* and *nosZ*, and followed an inverse pattern. The *napA* transcription started earlier than that of the other genes, increased quickly, and reached a maximum of 0.8 ± 0.2 mRNA copies * $cell^{-1}$, while the O_2 concentration was still above 5 µM in the liquid, 9.5 h post-inoculation (hpi). During this time, transcription of *nirK*, *norB* and *nosZ* stayed below 0.1–0.3 mRNA copies * $cell^{-1}$. When the O_2 decreased below 3 µM in the liquid at 14 hpi, the transcription of *napA* dropped to less than 0.1 mRNA copies * $cell^{-1}$, while the transcription of *nirK*, *norB* and *nosZ* reached maxima of 4.3 ± 1.6, 3.4 ± 0.7 and 6.8 ± 1.5 mRNA copies * $cell^{-1}$, respectively. At the same time, the cultures started rapid reduction of the exogenous N_2O. During this phase, NO and NO_2^- were transiently detected at low nanomolar concentrations, suggesting that the activity of NapAB, NirK and NorCB was very low. Transcription of *napA*, on the other hand, increased again and reached a second peak of 0.5 ± 0.1 mRNA copies * $cell^{-1}$ at 17 hpi. Inversely, transcription decreased to less than 0.2 mRNA copies * $cell^{-1}$ for *nirK* and *norB*, and 0.5 ± 0.1 mRNA copies * $cell^{-1}$ for *nosZ*. Matching

N_2O reduction and N_2 production rates, as well as the absence of NO_2^-, suggest that only the exogenous N_2O, but no NO_3^-, was reduced. When the exogenous N_2O was depleted at 21 hpi, NO_3^- reduction started, accompanied by a drop in *napA* transcription to less than 0.03 mRNA copies * $cell^{-1}$. The transcription of *nirK*, *norB* and *nosZ* reached a second peak with 1.2 ± 0.4, 0.9 ± 0.3 and 1.7 ± 0.7 mRNA copies * $cell^{-1}$, respectively. After approximately 3 h of NO_3^- reduction, the transcription of *napA* increased and reached a third peak with 0.3 ± 0.1 mRNA copies * $cell^{-1}$. This peak in *napA* transcription was followed by an increase in the NO_2^- concentration from less than 0.06 mM to 0.24 ± 0.03 mM. Such high micromolar concentrations of NO_2^- were not observed in other experiments that were less disturbed by sampling from the liquid phase. Towards the end of incubation, the transcription of all four denitrification genes declined, that of *napA* more rapidly than that of the others. Shortly after depletion of the NO_3^-, at 42 hpi, transcription of all genes was below 0.04 mRNA copies * $cell^{-1}$.

For comparison, a corresponding transcription analysis was done for cultures incubated under the same conditions but without exogenous N_2O, thus having only NO_3^- as an initial electron acceptor for denitrification (Fig. 2B, D, and F). The two treatments showed similar transcription patterns for all genes with respect to the initiation of transcription, where in both cases *napA* showed a different regulation than the other three genes. However, the pronounced dip in transcription of *nirK*, *norB* and *nosZ* at the time of O_2 depletion was less marked in cultures without exogenous N_2O, especially for the *nosZ* gene for which 1–2 transcripts $cell^{-1}$ were found until almost 30 hpi. Like in the N_2O treatments, NO_2^- accumulated at high micromolar concentrations towards the end of incubation.

NapAB is a weak competitor for electrons

A series of experiments was performed, aiming to impede the electron flow through the cytochrome bc_1 complex to cytochrome *c* and subsequently NirK, NorCB and NosZ. Injections of 15 μM myxothiazol or 100 μM antimycin A were tested. Antimycin A binds to the quinone reduction site of the cytochrome bc_1 complex, while myxothiazol binds to the quinol oxidation site. Injections took place shortly before O_2 depletion and the beginning reduction of exogenous N_2O. The treatment with 15 μM myxothiazol (Fig. 4C) partly inhibited the cytochrome bc_1 complex, seen from a NO_3^- reduction of 0.6 ± 0.1 μmol NO_3^--N * $flask^{-1}$ * h^{-1} in the presence of exogenous N_2O that was significantly higher ($p < 0.01$; *t*-test) than the ethanol negative control. The 15 μM myxothiazol treatments accumulated NO at nanomolar concentrations and NO_2^- to a concentration of 0.3 ± 0.2 mM during the reduction of the exogenous N_2O. The negative control showed no such accumulation of NO or NO_2^-. The 100 μM Antimycin A treatment (not shown) did not affect the electron flow to the cytochrome bc_1 complex, seen from a similar pattern of NO_3^- reduction as the negative control that received 0.75 ml of the solvent ethanol. The addition of 0.75 ml ethanol did slow down growth and gas production, but showed the same inhibition of NO_3^- reduction by N_2O as untreated cultures.

Another experiment was designed to bypass the electron flow through the cytochrome bc_1 complex with N,N, N′,N′-tetramethyl-p-phenylenediamine (TMPD), which can donate electrons directly to cytochrome *c* (Kimelberg and Nicholls, 1969; Bueno *et al*., 2009). This should stop the electron flow from quinol to the periplasmic cytochrome *c*, via the cytochrome bc_1 complex, making more electrons available to other quinol oxidases, like NapC. The TMPD was kept in a reduced state with an excess of 10 mM ascorbate. Cultures of AC87j1, treated with 100 μM TMPD, showed indeed a low but significant NO_3^- reduction rate of 0.9 ± 0.4 μmol NO_3^--N * $flask^{-1}$ * h^{-1} in the presence of exogenous N_2O (Fig. 4D). The effect of the TMPD on AC87j1 cultures varied substantially between flasks of a triplicate, as indicated by the high standard error in the NO_3^- reduction rate. While all three flasks reduced NO_3^- in the presence of exogenous N_2O, one flask reduced the added N_2O and NO_3^- within 31 h, another flask within 48 h (Fig. 4D) and the third flask within 85 h. For comparison, an untreated culture reduced the N_2O and NO_3^- within 20 h (Fig. 4A). The reason for a slow nitrogen metabolism could be an inefficient NO_2^-, NO and N_2O reduction, that does not yield a proton gradient, since the cytochrome bc_1 complex was bypassed with TMPD.

Growth rate and yield from exogenous N_2O and NO_3^- were identical

The optical density at 600 nm (OD_{600}) was measured regularly for strain AC87j1, grown anaerobically in YMB supplemented with 1 mM NO_3^- (50 μmol NO_3^-) and with or without 40 μmol N_2O (Supporting Information Fig. S3). The OD_{600} of both treatments was virtually identical until NO_3^- was close to depletion in the cultures without exogenous N_2O. Cultures with N_2O showed the same biphasic N_2 production as described above. Anaerobic growth from NO_3^-, with or without exogenous N_2O, yielded 6.1E7 ± 3E6 and 4.7E7 ± 1E6 cells at anaerobic growth rates of 0.055 ± 0.005 and 0.058 ± 0.002, respectively. Calculations that compensated for the different quantity of electron acceptor in treatments with and without exogenous N_2O showed that there was no significant difference in the number of electrons spent on NOx reduction per cell division ($p \geq 0.7$; t-Test). All treatments

Table 3. Statistics of the *Bradyrhizobium* strain AC87j1 genome.

	Bradyrhizobium strain AC87j1
# contigs	309
Size (Mb)	8.68 Mb
Average read coverage	7x
N_{50} (Kb)	71.5
% G + C	63.7
# RNAs	56
# coding sequences	8126
NCBI accession	PTFE00000000
NCBI BioProject	PRJNA419619

Information about the number of RNA genes and coding sequences were obtained from the prokaryotic genome automatic pipeline (PGAAP) annotation.

showed a yield of 1.9E11 $\pm$ 6.0E9 cells * mol^{-1} e^{-}, regardless of the electron acceptor being NO_3^- or N_2O.

Genes involved in nitrogen metabolism and electron transport in Bradyrhizobium *strain AC87j1*

The genome of *Bradyrhizobium* strain AC87j1 has a size of 8.7 Mb and a GC content of 64% (Table 3). It contains genes potentially encoding a fully functional denitrification pathway, comprised of periplasmic nitrate reductase NapAB, copper containing nitrite reductase NirK, cytochrome *c* dependent nitric oxide reductase NorCB and nitrous oxide reductase N_2OR. Genes coding for cytoplasmic dissimilatory nitrate reductase NarG were not identified in the genome. In addition to the four denitrification reductases, we found genes encoding assimilatory nitrate reductase NasA and assimilatory nitrite to ammonium reductase NirB, including various nitrate and nitrite transporters (Table 4).

For the electron supply to quinone in the cytoplasmic membrane, we found NADH dehydrogenase (EC 1.6.5.3, ubiquinone), NiFe hydrogenase, succinate dehydrogenase (EC 1.3.99.1) and several other respiratory dehydrogenases. NapAB receives electrons directly from quinol via membrane bound NapC; genes encoding NapGH were not found. Regarding electron transport to NirK, NorCB and NosZ, we found genes encoding the cytochrome bc_1 complex and the soluble periplasmic cytochromes c_2, c_4, c_{552} and c_{553}. No other cytochrome *c* reductase besides cytochrome bc_1 was found in the genome (Table 4).

We compared genes, and their translations, involved in denitrification and electron transport with those found in the well researched *B. diazoefficiens* USDA 110. The organization of the AC87j1 operons *napEDABC*, *nirK*, *norECBQD*, *nosRZDFYLX* and *fbcFH* matched those in USDA 110 closely. This includes characteristic features like FNR, FixK and/or NnrR consensus sequences, overlapping coding regions *napABC* and *nosDFYLX*, *fbcH* coding for cytochrome *b* and c_1, as well as signal peptides and protein motifs in translations. The translations of *napA*, *nirK*, *norC* and *nosZ* from AC87j1 showed 95%, 96%, 97% and 93% identity to the respective amino acid sequences from *B. diazoefficiens* USDA 110.

Discussion

Bradyrhizobia are commonly found among the dominating groups of bacteria reported from soil metagenomes (Souza *et al*., 2016; Castañeda and Barbosa, 2017). It is

Table 4. Overview of the gene inventory involved in denitrification in *Bradyrhizobium* strain AC87j1.

Gene	Size [bp]	Translation [AA]	AA identity to USDA 110 [%]	Function	GenBank accession
napE	186	61	95	Periplasmic nitrate reductase component NapE	PPQ19018.1
napD	315	104	85	Periplasmic nitrate reductase component NapD	PPQ19053.1
napA	2514	837	95	Periplasmic nitrate reductase (EC 1.7.99.4)	PPQ19017.1
napB	471	156	95	Nitrate reductase cytochrome c_{550}-type subunit	PPQ19016.1
napC	654	217	92	Cytochrome c-type protein NapC	PPQ19015.1
nirK	1098	365	96	Copper-containing nitrite reductase (EC 1.7.2.1)	PPQ18979.1
nirV	879	292	88	Nitrite reductase accessory protein NirV	PPQ18980.1
norE	579	192	89	Nitric oxide reductase subunit E	PPQ18322.1
norC	453	150	97	Nitric oxide reductase subunit C	PPQ18320.1
norB	1347	448	98	Nitric oxide reductase subunit B	PPQ18319.1
norQ	810	269	94	NorQ/CbbQ/NirQ/GpvN family protein	PPQ18318.1
norD	1917	638	91	NorD protein	PPQ18317.1
nosR	2298	765	70	N_2OR expression regulator NosR	PPQ18892.1
nosZ	1947	648	93	Nitrous oxide reductase (N_2OR), TAT-dependent (EC 1.7.99.6)	PPQ18891.1
nosD	1356	451	81	N_2OR maturation protein NosD, copper-binding	PPQ18890.1
nosF	921	306	58	N_2OR maturation protein NosF, copper ABC transporter	PPQ18889.1
nosY	828	275	70	N_2OR maturation transmembrane protein NosY	PPQ18888.1
nosL	573	190	54	N_2OR maturation outer-membrane lipoprotein NosL, copper chaperone	PPQ18887.1
nosX	996	331	50	N_2OR maturation periplasmic protein NosX	PPQ18886.1

therefore of general interest to acquire more knowledge about the regulation of denitrification in these organisms, and their potential roles as sinks/sources for N_2O. Most of the current knowledge on denitrification in bradyrhizobia is based on studies of *B. diazoefficiens* strain USDA 110 (Bueno *et al*., 2009; Sánchez *et al*., 2010; Torres *et al*., 2017), earlier classified as belonging to *B. japonicum*. Recent investigations showed that inoculation with genetically modified and wild-type strains of *B. diazoefficiens* could reduce N_2O emissions from soybean fields (Itakura *et al*., 2013; Akiyama *et al*., 2016). While rhizobia can denitrify inside nodules and thereby produce some N_2O (Mesa *et al*., 2004; Hirayama *et al*., 2011), most N_2O emitted from legume fields arises from the degradation of roots and other plant material by denitrifying bacteria in the soil (Akiyama *et al*., 2016). Finding ways to reduce the N_2O/N_2 product ratio by increasing the abundance of N_2O-reducing organisms could present an attractive option. Manipulations of the indigenous soil microflora seem, however, to be an unrealistic strategy. Instead, the increasing use of bacterial inoculants to improve the N_2-fixation of various legume crops offer a possibility to deliberately increase the N_2O-reducing portion of the denitrifying microbial community. In this work, we identified both complete and truncated denitrifiers that were distributed across the *Bradyrhizobium* phylogenetic tree, covering both the *B. japonicum* and *B. elkanii* superclades, and representing seven different genospecies (Fig. 1; Supporting Information Table S1). One strain, AC62a, reduced NO_3^- to NO but was unable to reduce it further. Rhizobia that have NO as end product for denitrification have been detected earlier (Falk *et al*., 2010). In the environment, organisms that can produce, but not reduce, NO probably live in consortia with organisms that carry NO reductase.

The complete denitrifiers mostly belonged to genospecies I in the *B. japonicum* superclade, but a few were found that belonged to genospecies II and IV. This is, to the best of our knowledge, the first report on widespread capacity for N_2O reduction among taxonomically diverse bradyrhizobia. Isolates that could not reduce N_2O were more evenly distributed over the tree and were also found in the *B. elkanii* superclade. The screening of denitrification end products thus revealed that, while all strains reduced NO_3^- to N_2O, only about 60 % of the denitrifying strains could reduce N_2O to N_2, meaning that the strains in this collection will act either as sources or sinks for N_2O. This highlights the necessity to determine the denitrification end products when searching for suitable inoculants for biofertilization in order to avoid strains that are unable to reduce N_2O, but it also shows that it is possible to identify a range of isolates, which can act as efficacious N_2 fixers in combination with suitable legume hosts, and at the same time efficiently mitigate N_2O emissions.

A major finding of our study was that the complete denitrifiers all showed a characteristic inhibition of NO_3^- reduction by exogenous N_2O (Fig. 2; Supporting Information Fig. S1). In soil, such strains would consume N_2O that was produced by surrounding organisms. This enhances the suitability of N_2 producing *Bradyrhizobium* strains for biofertilization tremendously. To elucidate the mechanisms behind this phenomenon, we performed a series of experiments based on detailed gas kinetics using strain AC87j1 as representative for all N_2 producing strains in this work. The results demonstrated clearly that N_2O inhibited NO_3^- reduction, even in the presence of functional NapAB. Experiments with inhibitors of the cytochrome bc_1 complex using myxothiazol (Fig. 4C) suggest that a competition between the respective electron transport routes to NapAB and NosZ was responsible for the inhibition of NO_3^- reduction by N_2O (Fig. 5). This was further supported by the experiment using TMPD which, by providing a surplus of electrons to NosZ via cytochrome *c*, allowed concomitant transfer of electrons to NapC directly from the cellular quinol pool (Fig. 4D). In *B. japonicum*, periplasmic NapAB receives electrons from membrane integrated NapC (Delgado *et al*., 2003), which in turn receives electrons from the quinol pool within the cytoplasmic membrane. In contrast, NirK, NorCB and NosZ all receive electrons from the cytochrome *c* pool in the periplasm (Otten *et al*., 1999); hence, the non-inhibition of NO_2^- reduction in the presence of N_2O. The cytochrome *c* is supplied with electrons from the quinol pool via membrane integrated cytochrome bc_1. We hypothesize that NO_3^- reduction in our *Bradyrhizobium* strains is less competitive for electrons than N_2O reduction due to several reasons (Fig. 5). The quinol oxidation site of the cytochrome bc_1 complex has a redox midpoint potential of +320 mV (Meinhardt *et al*., 1987), which is likely to be higher than that of the quinol oxidation site of NapC (Roldán *et al*., 1998). This thermodynamic advantage of the cytochrome bc_1 complex over NapC results in a higher electron flux from the quinol pool to the cytochrome bc_1 complex, and thus to the NO_2^-, NO and N_2O reductases. On the side of the substrates, the redox couple N_2O/N_2 has a higher redox midpoint potential than the couple NO_3^-/NO_2^-, with +1350 mV and + 421 mV, respectively. Again, this gives N_2O reduction a thermodynamic advantage over NO_3^- reduction. Last, but not least, the periplasmic cytochrome *c* pool might serve as a buffer for electrons from the quinol pool and transfer electrons more efficiently from the cytochrome bc_1 complex to NosZ, than NapC to NapAB (Sturm *et al*., 2015). A high concentration of cytochrome *c*, coupled with a potent cytochrome *c* oxidase in the form of NosZ, would lead to a more oxidized membrane and thus leave even less electrons from quinol available for NapC (Fig. 5). We hypothesize further that there are bacteria other than *Bradyrhizobium*, with periplasmic NapAB as the sole dissimilatory NO_3^- reductase and a similar electron transport pathway, that show an inhibition of NO_3^- reduction by N_2O.

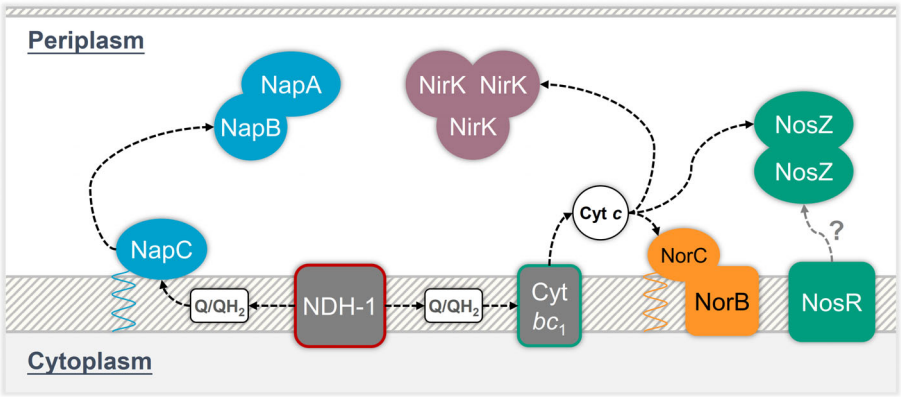

Fig. 5. Sketch of the electron transport in the plasma membrane and periplasm of *Bradyrhizobium* sp. NDH-1 represents NADH dehydrogenase 1 as electron source, which reduces quinone to quinol. Dashed arrows depict electron flow. Enzymes are placed according to their cellular localization, irrespective of their in vivo localization relative to each other or their possible association into a denitrification supercomplex (Borrero-de Acuña *et al*., 2016). The role of NosR as electron donor to NosZ has not been verified and therefore marked with a question mark.

The growth measurements (Supporting Information Fig. S3), showing identical growth rates from N_2O and from NO_3^-, demonstrated that the delivery of electrons, rather than differences between the involved electron acceptors, determined and limited growth in *Bradyrhizobium* under our experimental conditions. It is this limitation in the delivery of electrons to the cytoplasmic membrane that makes a metabolic control of denitrification possible. Additional electron pathways to NosZ, like NosR as speculated by Wunsch and Zumft (2005), could enhance the activity of NosZ further and also give N_2O reduction an advantage over NO_2^- and NO reduction by NirK and NorCB. However, in the absence of exogenous N_2O, cultures of AC87j1 accumulated NO_2^- at micromolar concentrations, while NO_3^- approached depletion, showing that NapAB can compete efficiently with NirK. The low nanomolar concentrations of NO in all experiments with NO_3^-, NO_2^- and N_2O suggest that NorCB reduces NO faster than it is provided by NO_2^- reduction through NirK.

Another reason for the preference for N_2O reduction over NO_3^- reduction could be that the number of reductase molecules differ. This cannot be ruled out by the present results, since the maximum transcript numbers of NosZ were almost nine times higher than for NapA (Fig. 2C-F). Transcription level is however only one contributing aspect determining the activity of an enzymatic reaction. The number of protein molecules produced per transcript varies between different genes (Liu *et al*., 2016), as do for example the turnover rate (K_{cat}) and affinity of the different enzymes. Elucidating to what extent these various factors contribute to the observed preference for N_2O reduction in these organisms will require further experimentation at the protein level.

The high-resolution gas kinetics in combination with transcription analysis during transition between aerobic and anaerobic respiration, and the following denitrification phase, provided novel aspects on the regulatory biology of denitrification in this group of organisms, exemplified by strain AC87j1. Previous work by other groups showed that transcription of denitrification genes in the model organism *Bradyrhizobium diazoefficiens* USDA 110 (earlier called *B. japonicum*) is regulated by the O_2 sensitive FixJL, the NO_3^--sensitive NasTS, the NO sensitive NnrR, the redox sensitive RegSR and the RegR and self-induced NifA (Torres *et al*., 2014; Cabrera *et al*., 2016). Noticeably, the expression of the *nap* and *nir* operons was apparently initiated by microoxic conditions, while that of the *nor* operon required a nitrogen oxide, probably NO (Bueno *et al*., 2017). Regulation of *nosZ* was not investigated, but another study (Torres *et al*., 2017) suggested microaerobic conditions as the main inducer of *nosZ*. Those findings are in stark contrast to those in the present study of strain AC87j, which showed that the regulation of *napA* differed significantly from that of *nirK*, *norB* and *nosZ*. The early transcription of *napA*, and the late transcription of *nirK*, *norB* and *nosZ* in the present study would explain the appearance of a low peak of NO_2^- at depletion of O_2. Simultaneously with the following transcription of *nirK*, *norB* and *nosZ*, the NO_2^- disappeared due to a faster reduction of NO_2^- than NO_3^-. With continuing transcription of *napA*, NO_2^- started to accumulate again. We hypothesize that the metabolic inhibition of NO_3^- reduction by N_2O balances denitrification in *Bradyrhizobium* AC87j1, thus avoiding the accumulation of NO_2^- and/or NO to cytotoxic concentrations. Incubations with 1 mM NO_2^- showed reduced respiration of both O_2 and the NO_2^- (Table 2). Incubations with 10 mM NO_3^- showed no adverse effect on gas kinetics, compared to incubations with 1 mM NO_3^-, suggesting that the higher NO_3^- concentration did not lead to more NO_2^- accumulation.

The second transcription peaks seen in the N_2O treatments (Fig. 2E) for transcription of *nirK*, *norB* and *nosZ* at 20 h, where *napA* transcription is at a second minimum, suggest that the redox state of the plasmamembrane, possibly sensed by the quinone binding RegS, is involved in the regulation of *nap*, *nir*, *nor* and *nos* transcription under anaerobic conditions. The downregulation events of *napA* transcription coinside with the depletion of O_2, and then that of exogenous N_2O. Considering quinone reductases as electron limiting components of aerobic and anaerobic respiration in AC87j1, the plasmamembrane is probably in an oxidized state in the

presence of preferable electron acceptors like O_2 and N_2O. Under anaerobic conditions, and in the presence of exogenous N_2O, an oxidized quinone pool could be an indirect signal for AC87j1 cells that N_2O reduction is outcompeting NO_3^- reduction, and that the cells can safely increase NO_3^- reduction by increasing transcription of *napA*. The depletion of the electron acceptor N_2O could then result in a sudden reduction of quionone to quinole, inducing transcription of *nirK*, *norB* and *nosZ*, and repressing *napA* transcription.

It remains to be elucidated if other organisms that denitrify NO_3^- to N_2 and reduce NO_3^- with periplasmic nitrate reductase, but lack the membrane-bond nitrate reductase NarG, show a similar behaviour. The feature makes such organisms very interesting from an environmental point of view, since they will act as net sinks for N_2O, blocking their own production of this gas as long as it is present in their surroundings, possibly produced by other denitrifying microorganisms. The results have potentially promising applications since these bacteria are nitrogen-fixing symbionts of many of the economically most important leguminous crops such as soybean and groundnut. Taking into account the increasing awareness that different combinations of bacterial strain/plant cultivar may vary largely in their nitrogen-fixing efficacy, our findings open the possibility to choose among a wide variety of candidates when searching for suitable inoculation strains that are not only efficient N_2 fixers with specific crop plants, but which in addition can act as potent N_2O reducers.

Ongoing and future work with different rhizobia, as well as non-rhizobial bacteria, will shed more light on the efficient N_2O reduction described for several *Bradyrhizobium* strains in this study, and establish whether it is unique to nitrate-reducing denitrifiers that use Nap, but not Nar, thus prove or disprove our hypothesis. It will also bring more information about how widespread the hampering NO_3^- reduction is among denitrifying bacteria.

Conclusions

The screening of denitrification phenotypes among taxonomically diverse isolates of *Bradyrhizobium* revealed that almost half of the isolates had a truncated denitrification pathway, lacking the capacity to reduce N_2O. Most others could denitrify NO_3^- to N_2 and showed a strong preference for N_2O over NO_3^-, resulting in rapid N_2O reduction. In-depth analysis suggested that this is due to a competition between the electron transport pathways to periplasmic NO_3^-- and N_2O reductases (Fig. 5). The findings provide novel information about transcriptional and metabolic control of denitrification in this ecologically and economically significant group of bacteria and highlight the need to consider N_2O reduction as an important trait, in addition to N_2-fixation efficacy, when developing new inoculants for legume production.

Acknowledgements

We thank Linda Bergaust for the genome sequencing and data treatment. This work was in parts financed by PASUSI within the ERA-NET Co-fund Horizon2020 program Leap-Agri, under the EC Grant agreement No. 727715 and Research Council of Norway project No. 290488. K. Woliy was supported by a grant from the Norwegian State Educational Loan Fund.

References

Akiyama, H., Hoshino, Y.T., Itakura, M., Shimomura, Y., Wang, Y., Yamamoto, A., *et al*. (2016) Mitigation of soil N_2O emission by inoculation with a mixed culture of indigenous *Bradyrhizobium diazoefficiens*. *Sci Rep* **6**: 1–8.

Altschul, S.F., Madden, T.L., Schäffer, A.A., Zhang, J., Zhang, Z., Miller, W., and Lipman, D.J. (1997) Gapped BLAST and PSI-BLAST: a new generation of protein database search programs. *Nucleic Acids Res* **25**: 3389–3402.

Aziz, R.K., Bartels, D., Best, A.A., DeJongh, M., Disz, T., Edwards, R.A., *et al*. (2008) The RAST server: rapid annotations using subsystems technology. *BMC Genomics* **9**: 75.

Bedmar, E.J., Robles, E.F., and Delgado, M.J. (2005) The complete denitrification pathway of the symbiotic, nitrogen-fixing bacterium *Bradyrhizobium japonicum*. *Biochem Soc Trans* **33**: 141–144.

Borrero-de Acuña, J.M., Rohde, M., Wissing, J., Schobert, M., Molinari, G., Timmis, K.N., *et al*. (2016) Protein network of the *Pseudomonas aeruginosa* Denitrification apparatus. *J Bacteriol* **198**: 1401–1413.

Bueno, E., Richardson, D.J., Bedmar, E.J., and Delgado, M. J. (2009) Expression of *Bradyrhizobium japonicum* cbb3 terminal oxidase under denitrifying conditions is subjected to redoxcontrol. *FEMS Microbiol Lett* **298**: 20–28.

Bueno, E., Robles, E.F., Torres, M.J., Krell, T., Bedmar, E.J., Delgado, M.J., and Mesa, S. (2017) Disparate response to microoxia and nitrogen oxides of the *Bradyrhizobium japonicum napEDABC*, *nirK* and *norCBQD* denitrification genes. *Nitric Oxide* **68**: 137–149.

Cabrera, J.J., Salas, A., Torres, M.J., Bedmar, E.J., Richardson, D.J., Gates, A.J., and Delgado, M.J. (2016) An integrated biochemical system for nitrate assimilation and nitric oxide detoxification in *Bradyrhizobium japonicum*. *Biochem J* **473**: 297–309.

Castañeda, L.E., and Barbosa, O. (2017) Metagenomic analysis exploring taxonomic and functional diversity of soil microbial communities in Chilean vineyards and surrounding native forests. *Peer J* **5**: 1–19.

Cox, R.D. (1980) Determination of nitrate and nitrite at the parts per billion level by chemiluminescence. *Anal Chem* **52**: 332–335.

Daniel, R.M., Limmer, a.W., Steele, K.W., and Smith, I.M. (1982) Anaerobic growth, nitrate reduction and denitrification in 46 *Rhizobium* strains. *Microbiology* **128**: 1811–1815.

Degefu, T., Wolde-meskel, E., Woliy, K., and Frostegård, Å. (2017) Phylogenetically diverse groups of *Bradyrhizobium*

isolated from nodules of tree and annual legume species growing in Ethiopia. *Syst Appl Microbiol* **40**: 205–214.

Delamuta, J.R.M., Ribeiro, R.A., Ormeño-Orrillo, E., Melo, I.S., Martínez-Romero, E., and Hungria, M. (2013) Polyphasic evidence supporting the reclassification of *Bradyrhizobium japonicum* group Ia strains as *Bradyrhizobium diazoefficiens* sp. nov. *Int J Syst Evol Microbiol* **63**: 3342–3351.

Delgado, M.J., Bonnard, N., Tresierra-Ayala, A., Bedmar, E. J., and Müller, P. (2003) The *Bradyrhizobium japonicum napEDABC* genes encoding the periplasmic nitrate reductase are essential for nitrate respiration. *Microbiology* **149**: 3395–3403.

Falk, S., Liu, B., and Braker, G. (2010) Isolation, genetic and functional characterization of novel soil *nirK*-type denitrifiers. *Syst Appl Microbiol* **33**: 337–347.

Frunzke, K., and Zumft, W.G. (1986) Inhibition of nitrous-oxide respiration by nitric-oxide in the denitrifying bacterium *Pseudomonasperfectomarina*. *Biochim Biophys Acta* **852**: 119–125.

Herridge, D.F., Peoples, M.B., and Boddey, R.M. (2008) Global inputs of biological nitrogen fixation in agricultural systems. *Plant and Soil* **311**: 1–18.

Hirayama, J., Eda, S., Mitsui, H., and Minamisawa, K. (2011) Nitrate-dependent N_2O emission from intact soybean nodules via denitrification by *Bradyrhizobium japonicum* bacteroids. *Appl Environ Microbiol* **77**: 8787–8790.

Itakura, M., Uchida, Y., Akiyama, H., Hoshino, Y.T., Shimomura, Y., Morimoto, S., *et al*. (2013) Mitigation of nitrous oxide emissions from soils by *Bradyrhizobium japonicum* inoculation. *Nat Clim Chang* **3**: 208–212.

Kimelberg, H.K., and Nicholls, P. (1969) Kinetic studies on the interaction of TMPD with cytochrome c and cytochrome c oxidase. *Arch Biochem Biophys* **133**: 327–335.

Liu, Y., Beyer, A., and Aebersold, R. (2016) On the dependency of cellular protein levels on mRNA abundance. *Cell* **165**: 535–550.

MacArthur, P.H., Shiva, S., and Gladwin, M.T. (2007) Measurement of circulating nitrite and S-nitrosothiols by reductive chemiluminescence. *J Chromatogr B* **851**: 93–105.

Meinhardt, S.W., Yang, X.H., Trumpower, B.L., and Ohnishi, T. (1987) Identification of a stable ubisemiquinone and characterization of the effects of ubiquinone oxidation-reduction status on the Rieske iron-sulfur protein in the three-subunit ubiquinol-cytochrome c oxidoreductase complex of *Paracoccus denitrificans*. *J Biol Chem* **262**: 8702–8706.

Mesa, S., Velasco, L., Manzanera, M.E., Delgado, M.J., and Bedmar, E.J. (2002) Characterization of the *norCBQD* genes, encoding nitric oxide reductase, in the nitrogen fixing bacterium *Bradyrhizobium japonicum*. *Microbiology* **148**: 3553–3560.

Mesa, S., Bedmar, E.J., Chanfon, A., Hennecke, H., and Fischer, H. (2003) *Bradyrhizobium japonicum* NnrR, a Denitrification regulator, expands the FixLJ-FixK2 regulatory cascade. *J Bacteriol* **185**: 3978–3982.

Mesa, S., De Dios Alché, J., Bedmar, E.J., and Delgado, M. J. (2004) Expression of *nir*, *nor* and *nos* denitrification genes from *Bradyrhizobium japonicum* in soybean root nodules. *Physiol Plant* **120**: 205–211.

Molstad, L., Dörsch, P., and Bakken, L.R. (2007) Robotized incubation system for monitoring gases (O_2, NO, N_2O N_2) in denitrifying cultures. *J Microbiol Methods* **71**: 202–211.

Montzka, S.A., Dlugokencky, E.J., and Butler, J.H. (2011) Non-CO_2 greenhouse gases and climate change. *Nature* **476**: 43–50.

Otten, M.F., Reijnders, W.N.M., Bedaux, J.J.M., Westerhoff, H.V., Krab, K., and Van Spanning, R.J.M. (1999) The reduction state of the Q-pool regulates the electron flux through the branched respiratory network of *Paracoccus denitrificans*. *Eur J Biochem* **261**: 767–774.

Overbeek, R., Olson, R., Pusch, G.D., Olsen, G.J., Davis, J. J., Disz, T., *et al*. (2014) The SEED and the rapid annotation of microbial genomes using subsystems technology (RAST). *Nucleic Acids Res* **42**: 206–214.

Ramírez-Bahena, M.-H., Velázquez, E., Fernández-Santos, F., Peix, A., Martínez-Molina, E., and Mateos, P. F. (2009) Phenotypic, genotypic, and symbiotic diversities in strains nodulating clover in different soils in Spain. *Can J Microbiol* **55**: 1207–1216.

Reay, D.S., Davidson, E.A., Smith, K.A., Smith, P., Melillo, J.M., Dentener, F., and Crutzen, P.J. (2012) Global agriculture and nitrous oxide emissions. *Nat. Clim. Chang.* **2**: 410–416.

Rogelj, J., Shindell, D., Jiang, K., Fifita, S., Forster, P., Ginzburg, V., et al. (2018) Mitigation pathways compatible with 1.5°C in the context of sustainable development. In, V. Masson-Delmotte, P. Zhai, H. O. Pörtner, D. Roberts, J. Skea, P.R. Shukla, A. Pirani, W. Moufouma-Okia, C. Péan, R. Pidcock, S. Connors, J. B. R. Matthews, Y. Chen, X. Zhou, M. I. Gomis, E. Lonnoy, T. Maycock, M. Tignor, and T. Waterfield. (ed), *Global Warming of 1.5°C. An IPCC Special Report on the impacts of global warming of 1.5°C above pre-industrial levels and related global greenhouse gas emission pathways, in the context of strengthening the global response to the threat of climate change, sustainable development, and efforts to eradicate poverty*. In Press

Roldán, M.D., Sears, H.J., Cheesman, M.R., Ferguson, S.J., Thomson, a.J., Berks, B.C., and Richardson, D.J. (1998) Spectroscopic characterization of a novel multiheme c-type cytochrome widely implicated in bacterial electron transport. *J Biol Chem* **273**: 28785–28790.

Sánchez, C., Gates, A.J., Meakin, G.E., Uchiumi, T., Girard, L., Richardson, D.J., *et al*. (2010) Production of nitric oxide and nitrosylleghemoglobin complexes in soybean nodules in response to flooding. *Mol Plant Microbe Interact* **23**: 702–711.

Schwartz, W. (1972) J. M. Vincent, a manual for the practical study of the root-nodule bacteria (IBP Handbuch no. 15 des international biology program, London). XI u. 164 S., 10 Abb., 17 tab., 7 Taf. Oxford-Edinburgh 1970: Blackwell scientific Publ., 45 s. *Z Allg Mikrobiol* **12**: 1521–4028.

Shapleigh, J.P. (2013) The prokaryotes: prokaryotic physiology and biochemistry. In *The prokaryotes*, Rosenberg, E., DeLong, E.F., Lory, S., Stackebrandt, E., and Thompson, F. (eds). Berlin, Heidelberg: Springer Berlin Heidelberg, pp. 405–425.

Siqueira, A.F., Minamisawa, K., and Sánchez, C. (2017) Anaerobic reduction of nitrate to nitrous oxide is lower in *Bradyrhizobium japonicum* than in *Bradyrhizobium diazoefficiens*. *Microbes environ* **32**: 398–401.

Souza, R.C., Mendes, I.C., Reis-Junior, F.B., Carvalho, F. M., Nogueira, M.A., Vasconcelos, A.T.R., *et al*. (2016) Shifts in taxonomic and functional microbial diversity with agriculture: how fragile is the Brazilian Cerrado? *BMC Microbiol* **16**: 1–15.

Sturm, G., Richter, K., Doetsch, A., Heide, H., Louro, R.O., and Gescher, J. (2015) A dynamic periplasmic electron

transfer network enables respiratory flexibility beyond a thermodynamic regulatory regime. *ISME J* **9**: 1802–1811.
Thrall, P.H., Laine, A., Broadhurst, L.M., Bagnall, D.J., and Brockwell, J. (2011) Symbiotic effectiveness of rhizobial mutualists varies in interactions with native Australian legume genera. *PLoS Med* **6**: 1–11.
Torres, M.J., Argandoña, M., Vargas, C., Bedmar, E.J., Fischer, H.-M., Mesa, S., and Delgado, M.J. (2014) The global response regulator RegR controls expression of denitrification genes in *Bradyrhizobium japonicum*. *PLoS One* **9**: e99011.
Torres, M.J., Bueno, E., Jiménez-Leiva, A., Cabrera, J.J., Bedmar, E.J., Mesa, S., and Delgado, M.J. (2017) FixK2 is the main transcriptional activator of *Bradyrhizobium diazoefficiens nosRZDYFLX* genes in response to low oxygen. *Front Microbiol* **8**: 1–16.
Tucker, K.D., and Neal, J.L. (1988) Growth and respiration of *Bradyrhizobium japonicum* USDA 143 with nitrous oxide as the terminal electron acceptor. *Curr Microbiol* **17**: 89–94.
Untergasser, A., Nijveen, H., Rao, X., Bisseling, T., Geurts, R., and Leunissen, J.a.M. (2007) Primer3Plus, an enhanced web interface to Primer3. *Nucleic Acids Res* **35**: W71–W74.
Velasco, L., Mesa, S., Delgado, M.J., and Bedmar, E.J. (2001) Characterization of the *nirK* gene encoding the respiratory, cu-containing nitrite reductase of *Bradyrhizobium japonicum*. *Biochim Biophys Acta - Gene Struct Expr* **1521**: 130–134.
Velasco, L., Mesa, S., Xu, C.A., Delgado, M.J., and Bedmar, E.J. (2004) Molecular characterization of *nosRZDFYLX* genes coding for denitrifying nitrous oxide reductase of *Bradyrhizobium japonicum*. *Antonie van Leeuwenhoek, Int J Gen Mol Microbiol* **85**: 229–235.
Vinuesa, P., Rojas-Jiménez, K., Contreras-Moreira, B., Mahna, S.K., Prasad, B.N., Moe, H., *et al*. (2008) Multilocus sequence analysis for assessment of the biogeography and evolutionary genetics of four Bradyrhizobium species that nodulate soybeans on the asiatic continent. *Appl Environ Microbiol* **74**: 6987–6996.
Wolde-Meskel, E., Berg, T., Peters, N.K., and Frostegård, Å. (2004) Nodulation status of native woody legumes and phenotypic characteristics of associated rhizobia in soils of southern Ethiopia. *Biol Fertil Soils* **40**: 55–66.
Wolde-meskel, E., Terefework, Z., Lindström, K., and Frostegård, Å. (2004a) Rhizobia nodulating African *Acacia* spp. and *Sesbania sesban* trees in southern Ethiopian soils are metabolically and genomically diverse. *Soil Biol Biochem* **36**: 2013–2025.
Wolde-meskel, E., Terefework, Z., Lindström, K., and Frostegård, Å. (2004b) Metabolic and genomic diversity of rhizobia isolated from field standing native and exotic woody legumes in southern Ethiopia. *Syst Appl Microbiol* **27**: 603–611.
Wolde-Meskel, E., Terefework, Z., Frostegård, Å., and Lindström, K. (2005) Genetic diversity and phylogeny of rhizobia isolated from agroforestry legume species in southern Ethiopia. *Int J Syst Evol Microbiol* **55**: 1439–1452.
Wunsch, P., and Zumft, W.G. (2005) Functional domains of NosR, a novel transmembrane iron-sulfur flavoprotein necessary for nitrous oxide respiration. *J Bacteriol* **187**: 1992–2001.
Yang, L., and Cai, Z. (2005) The effect of growing soybean (*Glycine max*. L.) on N_2O emission from soil. *Soil Biol Biochem* **37**: 1205–1209.

Supporting Information

Additional Supporting Information may be found in the online version of this article at the publisher's web-site:

Fig. S1. Gas kinetics for five *Bradyrhizobium* strains during and after transition from aerobic respiration to denitrification. The cultures were incubated in YMB, supplemented with 1 mM NO_3^- (50 μmol) and with 1 ml initial O_2 in the headspace (~10 μM in the liquid), and 40 μmol initial N_2O. Strain names are given in the corresponding diagrams, and genospecies are given in parentheses. Incubations were conducted in duplicates. All strains showed the same, characteristic two-phased N_2 production with high rates during reduction of the exogenous N_2O and lower rates when cells shifted to reduction of NO_3^- to N_2, as shown for strain AC87j1 (Fig. a).
Fig. S2. Gas kinetics for five *Bradyrhizobium* strains during and after transition from aerobic respiration to denitrification. The cultures were incubated in YMB, supplemented with 1 mM NO_3^- (50 μmol) and with 1 ml initial O_2 in the headspace (~10 μM in the liquid), and 40 μmol initial N_2O. Strain names are given in the corresponding diagrams, and genospecies are given in parentheses. Incubations were conducted in duplicates. Strains AC87b3 and AC8 7 l produced N_2 only slowly and did not reduce all of the supplemented N_2O and NO_3^- within 100 h after O_2 depletion. Of the remaining three strains, at least one duplicate produced NO at micromolar concentrations. Due to the incubation in batch cultures, the NO inhibited N_2OR, or even growth of the cultures. * Full reduction of NO_x to N_2 was confirmed by two measurements at 250 and 320 h post inoculation.
Fig. S3. Growth curves of Bradyrhizobium strain AC87j1 incubated in YMB, supplemented with 1 mM NO_3^-, and with or without approximately 40 μmol initial N_2O in the headspace. Growth was measured as optical density at 600 nm (OD_{600}). Error bars show standard deviation for triplicate incubations.
Table S1. End-products of denitrification in *Bradyrhizobium* strains from this study.